Elasticity of Poly(azobenzene−peptides)

Gregor Neuert,[†,‡] Thorsten Hugel[⊥,‡,§] Roland R. Netz,[‡,§] and Hermann E. Gaub*[,†,‡]

Lehrstuhl für Angewandte Physik, Center for Nanoscience, Ludwig-Maximilians-Universität, Amalienstrasse 54, 80799 München, Germany, and Physics Department, Zentralinistitut für Medizintechnik TU-München, 85748 Garching, Germany

Received July 25, 2005; Revised Manuscript Received October 31, 2005

ABSTRACT: Since the mechanical properties of individual polymers have become accessible with single molecule force spectroscopy, detailed insight was gained into the molecular origin of their elasticity. Active, optically switchable polymers were introduced as photonic muscles and used in single molecule motors. Here, we present experimental data and calculations to describe the mechanical properties of poly(azobenzene−peptides) in the complete force regime accessible by AFM. The high force regime is very well described by ab initio quantum mechanical calculations, while for the low force regime we combine ab initio calculations with a description of the entropic forces based on the freely rotating chain model. Finally, a one-parameter fit for the different configurations of the poly(azobenzene−peptide) and a quantitative description of the optically induced actuation are given.

Introduction

Single molecule force spectroscopy has provided a very detailed insight into the mechanics of individual polymers. Proteins were unfolded,[1−5] nucleic acids were unzipped,[6−13] and synthetic polymers were disentangled[14−18] and peeled from surfaces.[14,19−21] Interactions within and between molecules were analyzed and quantified with unparalleled resolution and sensitivity. Different techniques evolved for different applications. Optical traps,[11,22−26] magnetic tweezers,[11,12] and vesicle pipet[27−29] techniques have been optimized for low force applications in the range well below 100 pN at the expense of spatial resolution and dynamic range. Cantilever-based techniques with their subnanometer spatial resolution were found to be ideally suited for applications starting from several piconewtons (pN) up to the nanonewton (nN) regime, where covalent bond rupture occurs.[14,30−34]

At low forces the intramolecular conformations of polymers are found to be governed by entropic effects, whereas at high forces the backbone deformations prevail.[35] The crossover regime was found to be dominated by supramolecular rearrangements such as folding in proteins,[1,3] hybridization on nucleic acids,[6,9,36,37] or solvent interactions.[34] This regime provided a richness of fingerprints specific for the chemical nature of the polymer and its particular material properties or its biological function.[1,3,6,15,16,18,34,38]

The elastic response of simple polymers with negligible supramolecular rearrangements was in the past successfully modeled by either the wormlike chain (WLC) model[3,5,13,14,39,40] or the freely jointed chain (FJC) model,[14,34,40,41] both with modifications to account for the backbone elasticity and the resulting softening at higher forces. Recently, a parameter-free description of the elasticity of four standard polymers—polypeptides, poly(nucleic acid), poly(ethylene glycol), and polyvinylamine—based on a combination of statistical mechanics and quantum mechanics was introduced.[35,42] The backbone elasticity, which dominates the elastic response of the polymers at higher forces, was calculated with ab initio quantum mechanical (QM) methods.[35,40,43−46] The low force contributions were described by the freely rotating chain (FRC) model.[40,43] As a result, a convincing fit of experimental force−extension curves in a force regime from 10 pN to 2 nN was obtained for polyvinylamine. These studies were partly motivated by findings that weak interaction of the polymer with the solvent as low as 1 k_BT per monomer unit could be determined, and that the accuracy was limited more by the quality of the model than by the precision of the experimental data.[4,34,43]

In addition, single polymers are the ultimate milestone in miniaturization of materials, and in combination with molecular actuators, of active devices. In a previous study we had shown that a single poly(azobenzene−peptide) might be operated in a repetitive expansion contraction cycle, in close analogy to an Otto cycle.[15,16] The action may also be seen as a photonic muscle, converting optical energy into mechanical work upon contraction. Such optically driven devices are generally regarded as promising candidates for the realization of nanoscale motors, since optical agitation and fueling offer striking advantages in both speed and versatility, compared to electrical wiring or slow diffusive transport of chemicals.[47−59] In the previous study the precision of the data analysis was largely hampered by the empiric model used for the fit of the force−extension curves before and after optical switching.[16] The quantum efficiency of the opto-mechanical conversion, which is the major target for further improvement in applications of this system as photonic muscle, could only be estimated on the basis of relative measurements.[15,16] Hence, a parameter-free fit of the force−extension curves as a function of the number of *cis*- and *trans*-azobenzene units is clearly a desirable goal.

In the present paper we combine experimental results for the force−distance behavior of polyazobenzene molecules with ab initio results for the large-force stretching behavior and a statistical-mechanical description of conformational fluctuations in the low-force range. The successful fitting of the experimental data allows a detailed analysis of the light-induced isomeric state of the azobenzene compound.

Our previous experimental studies revealed an unexpectedly high potential barrier between the cis and the trans conformation,

* To whom correspondence should be addressed: e-mail gaub@physik.uni-muenchen.de.
† Lehrstuhl für Angewandte Physik.
‡ Center for Nanoscience.
§ Physics Department.
⊥ Zentralinistitut für Medizintechnik TU-München.

10.1021/ma051622d CCC: $33.50
Published on Web 12/15/2005

indicating that the thermally activated conversion pathway between the two conformations is not collinear with the forced pathway.[16,60] Our quantum chemical calculations of the molecular conformations under external mechanical tension in fact lead to further insights with respect to the forced transition pathway. We demonstrate that the mechanical stretching modulus of the transition state is an important parameter which describes to what degree the conversion between two molecular states is stimulated or slowed down by the action of external forces. We believe that this finding applies quite generally and might be of importance for other systems as well.

Experimental Section

Sample Preparation. The azobenzene−tripeptide building block was synthesized as described in refs 16 and 61; it was then polymerized and functionalized on the N-terminus with a trityl-protected cystein.[15,16] For the attachment onto the cantilever, the nonpolar poly(azobenzene−peptide) was dissolved in dimethyl sulfoxide (DMSO) and physisorbed on a cantilever tip (Microlevers, Park Scientific Instruments, Sunnyvale, CA), which was evaporated with 0.5 nm CrNi and 50 nm gold.[15] The trityl-protected thiol group of the cystein was deprotected with trifluoroacetic acid/CH_2Cl_2, resulting in chemisorption of the poly(azobenzene−peptide) to the tip via the formation of a covalent Au−S bond. The C-terminal end of the polymer was coupled in situ to a flint glass slide (Schott), previously amino-functionalized by silanization with *N*′-[3-(trimethoxysilyl)propyl]diethylene−triamine (Aldrich).[38] The amide bond was formed in the presence of 100 mM *N*-hydroxysuccinimid (NHS) and 1-ethyl-3-(3-(dimethylamine)propyl)carbodiimide (EDC) (NHS and EDC in 1:1 molar ratio) in DMSO.[15,16]

The nonpolar homobifunctional C-(GVGVP)nx251-C polypeptide (kindly provided by Dan Urry) was immobilized on a gold-coated glass slide by incubation and picked up with a gold-coated cantilever tip (Olympus Biolever). [17] Both the Si_3N_4 cantilever tips and the glass slide were evaporated with 0.5 nm CrNi and 30 nm gold.[17] These measurements were performed in Millipore water and at room temperature.[15]

Optical switching of the poly(azobenzene−peptide) was achieved by coupling light from a xenon flash lamp (Rapp OptoElectronic, Hamburg, Germany) into the polished flint glass slide (F-2, Schott Glass Mainz, Hellma Optic GmbH, Jena, Germany, $n_D = 1.666$) via total internal reflection (TIR). A band-pass filter at 365 nm (fwhm 12.2 nm) and a filter setup at 430 nm (high pass GG420 in combination with BG 12) were placed between the flash lamp and the flint glass slide to excite the azobenzene unit and switch between the cis and the trans conformation. To achieve high transmission in the UV, it was necessary to use flint glass slides. DMSO (Aldrich, München, Germany, $n_D = 1.48$) was used as a solvent.[15,16]

The technique of atomic force microscopy (AFM)-based force spectroscopy and the instrumental setup have been described in detail elsewhere.[15,16,30,35,62] The cantilever tips used in our experiments had spring constants of 5, 12, and 35 mN m^{-1}. The spring constant of each cantilever was individually calibrated by measuring the amplitude of its thermal oscillations.[63] The sensitivity of the optical lever detection was measured by indenting the cantilever tip into a hard surface.

Data Collection and Analysis. The data collection and correction of the traces analyzed in this paper are described in detail elsewhere.[16] Stretching the same molecule several times in series made it possible to average over three to five force curves, resulting in an improved signal-to-noise ratio. The averaged force curves were smoothed by a three-point sliding average procedure before fitting.

Theoretical Description

Ab Initio Quantum Mechanical Model. In the past years the mechanical response of single molecules under stretching forces has been extensively investigated with ab initio quantum chemistry.[35,40,43−46,64] Ab initio methods are performed at zero temperature and therefore miss entropic effects due to conformational fluctuations. These fluctuations become irrelevant at high stretching forces. Therefore, ab initio methods become very accurate at high stretching force. We have recently shown how to combine entropic effects, embodied in the freely rotating chain model, with ab initio predictions and achieved a fit function for polyvinylamine in the whole force range accessible by AFM.[35] In this section we present results for azobenzene molecules under tension. As described before, azobenzene exists

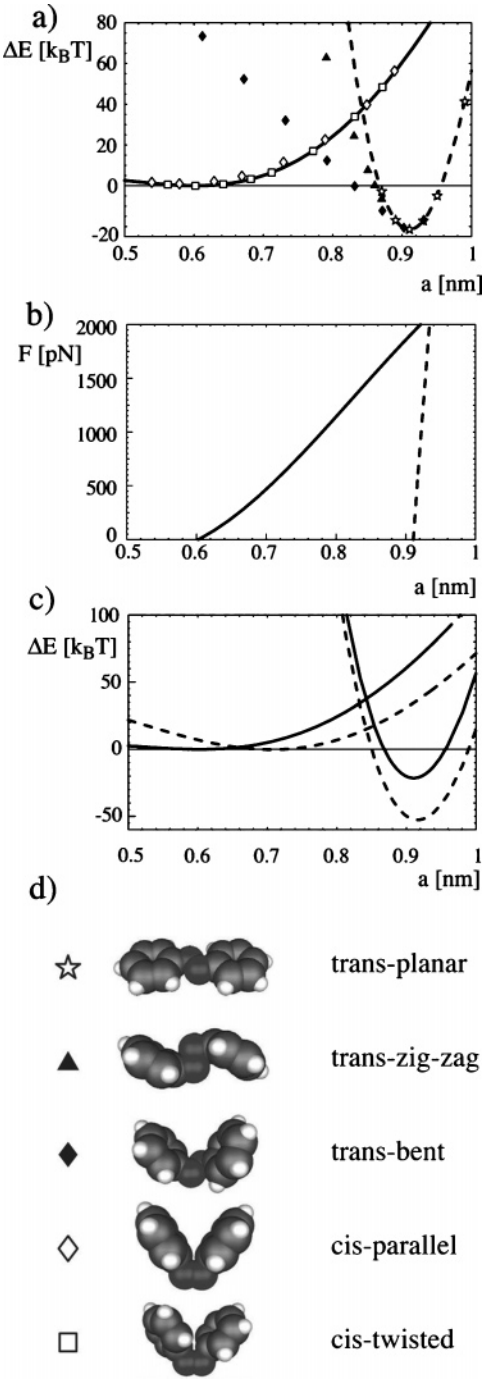

Figure 1. Force-dependent energy landscape of azobenzene. (a) Energies of different locally stable configurations as a function of the distance, *a*, between the two outer carbon atoms. The solid line denotes fits of the cis-twisted and the trans-planar conformation (dashed line). (b) Force−extension curves of the cis-twisted conformation (solid line) and the trans-planar conformation (dashed line). (c) Plot of the energy curves for the cis and trans state in the absence of force (solid lines) and in the presence of an external force of 500 pN (broken line). (d) Different configurations are trans-planar (open stars), trans-zigzag (filled triangles), trans-bent (filled diamonds), cis-parallel (open diamonds), and cis-twisted (open squares).

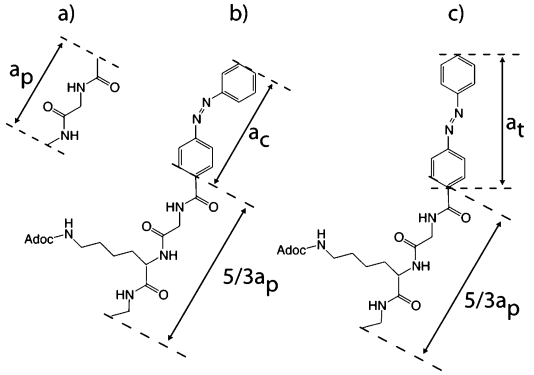

Figure 2. Chemical structures of a nonpolar dipeptide (a) and the nonpolar azobenzene tripeptide in the cis (b) and the trans (c) conformation. For the FRCQM-fits, the polymer is separated into building blocks of *cis*-azobenzene (unit length $a_c = 0.6027$ nm), *trans*-azobenzene (unit length $a_t = 0.9106$ nm), and tripeptide (unit length $^5/_3 a_p = 1.2166$ nm).

in a trans and cis conformation.[60] By performing an unconstrained geometry search for a single azobenzene unit, we identified even further local minima conformations. In Figure 1a we show the energy of five different conformations as a function of the distance between the two outer carbon atoms.

For convenience, we measure all energies relative to the ground-state energy of the cis-twisted conformation.

In ab initio methods one obtains the ground-state energy of a certain molecular configuration on the basis of the Schrödinger equation, within various numerical approximation schemes. In Hartree−Fock methods, the electron distribution is evaluated on the mean-field level; i.e., each electron sees an average density distribution due to the other electrons, and correlations are neglected. To numerically solve the many-electron problem on the computer, an additional approximation must be made, and the density distribution is expanded in a necessarily incomplete set of basis functions. In the present paper, all calculations are performed on the quite restricted level of Slater-type-orbitals with six Gaussian functions (STO-6G).[35,44] However, our estimated cis−trans energy difference, which is of the order of 21 k_BT, compares quite well with experimental measurements which find this energy difference to be of the order of 17−20 k_BT.[65] In previous calculations, we have shown that although the absolute energy difference between different basis sets can be considerable, forces depend significantly less on basis set quality (and on including electronic correlations) since they correspond to energy differences.[35,44] All different conformations are quite stable, meaning that they are separated by large barriers in the multidimensional conformation space (which we will discuss later on). The geometries are schematically depicted in Figure 1d. For further analysis, we concentrate on the cis-twisted conformation and on the trans-planar conformation (note that the trans-zigzag conformation and the trans-bent conformation become degenerate with the trans-planar conformation at distances larger than the equilibrium distance in the trans conformation, which means under extensional forces). The lines in Figure 1a denote polynomial fits for trans (dashed line) and cis (solid line) conformations according to the formula

$$\Delta E = \sum_{n=0}^{\infty} c_n a^{n+1}/(n+1) \tag{1}$$

where a denotes the distance between the outer carbon atoms in the azobenzene unit. All energies are measured relative to the ground state of the cis state. The choice of unit cell reflects the chemistry of the used azobenzene molecules, where spacer groups (peptide units) are linked to the azobenzene extremities (Figure 2).

Table 1. All Elastic Constants Obtained from the ab-Initio Calculation for a Unit Cell of Azobenzene in the Cis and in the Trans Conformation

	c_0 (nN)	c_1 (nN/nm)	c_2 (nN/nm^2)	c_3 (nN/nm^3)	a_0 (nm)
trans-azobenzene	−826.66	2,342.8	−2,254.2	745.0	0.9106
cis-azobenzene	9.992	−45.93	64.35	−25.942	0.6027

Table 2. Rescaled Elastic Constants Obtained from the ab-Initio Calculation for a Unit Cell of Azobenzene in the Cis and in the Trans Conformation

	d_0 (nN)	d_1 (nN)	d_2 (nN)	d_3 (nN)	a_0 (nm)
trans-azobenzene	−826.66	2,133.9	−1,869.1	562.49	0.9106
cis-azobenzene	9.992	−27.689	23.378	−5.68	0.6027

Our fitting results for the elastic coefficients c_n are given in Table 1. The experimentally measurable quantity is the force, which follows from eq 1 by a derivative

$$F = \frac{\partial \Delta E}{\partial a} = \sum_{n=0}^{\infty} c_n a^n \tag{2}$$

and is shown in Figure 1b for the trans (dashed line) and cis (solid line) conformations. The equilibrium extension follows from eq 2 by setting $F = 0$ and is denoted by a_0. Note that eq 2 gives the force of a single azobenzene unit, which can be generalized for a polymer of arbitrary length by writing

$$F = \sum_{n=0}^{\infty} d_n (a/a_0)^n = \sum_{n=0}^{\infty} d_n (L/L_0)^n \tag{3}$$

where $d_n = (a_0)^n c_n$. The results for the coefficients d_n are given in Table 2. Yet another way of expressing the force response is obtained by reexpanding eq 3 around the equilibrium length, leading to the expression

$$F = \sum_{n=1}^{\infty} \gamma_n (a/a_0 - 1)^n \tag{4}$$

Two mechanisms of conversion between the cis and trans have been discussed in the literature, namely the in-plane inversion of the N−N double bond and the rotation around the dihedral angle.[60] Our results in Figure 1a show that the inversion path way is faced with an activation barrier with a height of at least 35 k_BT (note that the crossing of the two locally stable conformational branches does not correspond to the true transition state, which most likely is of higher energy). It is important to note that the cis state is much softer than the trans state and thus yields quite easily to extensional forces. This is demonstrated in Figure 1c, where we plot the energy curves for the cis and trans state in the absence of force (solid lines) and in the presence of an external force of 500 pN (broken line). It is seen that the length of the cis state increases substantially in the presence of an external force, and as a result, the barrier decreases less than it would in the absence of elasticity effects. For a force of 500 pN, the barrier height has decreased to 20 k_BT. Experimentally, there is evidence that the actual conversion pathway involves a rotation of the N−N dihedral bond angle.[66] Therefore, we study the rotation under extensional force in the following.

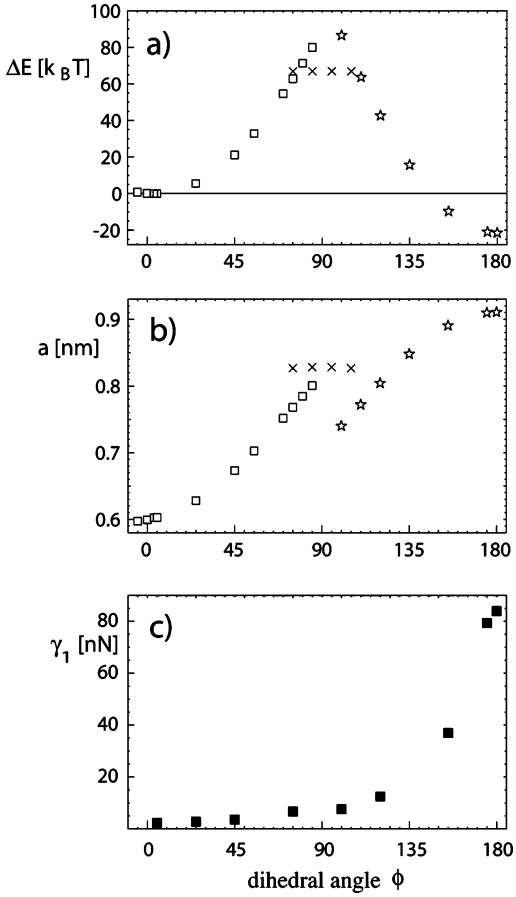

Figure 3. Transition between the cis and trans conformation is visualized by a rotation around the dihedral angle ϕ at the nitrogen−nitrogen bond by 180°. (a) The energy as a function of this angle is plotted. The cis-twisted geometry (denoted by squares) becomes instable at dihedral angles above roughly $\phi = 85°$. Likewise, the trans conformation (star) loses stability at angles below $\phi = 105°$. At the crossover between the cis and trans conformation, an intermediate structure (cross) appears. This demonstrates that close to the barrier many competing and locally stable structures exist. (b) The distance between the two outer carbon atoms as a function of the dihedral angle ϕ is plotted for the cis conformation (squares), the trans conformation (star), and the intermediate stae (cross). The unit cell size of the barrier state is roughly intermediate between the unit cell size in the cis and trans conformations. (c) The stretching modulus of the azobenzene as a function of the dihedral angle is plotted. It is seen that as the dihedral angle increases, the molecules becomes stiffer, meaning that in the cis conformation the molecule easily yields to the externally applied force.

The transition between cis and trans conformations can be visualized by a rotation around the dihedral angle ϕ at the nitrogen−nitrogen bond by 180°. In Figure 3a we show the energy as a function of this angle.

In the calculation, we have only fixed the dihedral angle but have otherwise optimized the geometry of the whole molecule. The distance between the two outer carbon atoms as a function of the dihedral angle is plotted in Figure 3b. In Figure 3c, the stretching modulus γ_1 of the azobenzene as a function of the dihedral angle is plotted.

Further, we investigated the influence of force on the energy as a function of the angle ϕ. The force-dependent energy for $F = 0$ nN, $F = 0.5$ nN, and $F = 1$ nN is calculated by eq 5 and shown in Figure 4a.

$$\Delta\tilde{E}(F) = \Delta E - (a[\phi] - a_{0,\mathrm{cis}})F \tag{5}$$

In Figure 4b we include the stretching modulus γ_1 of the azobenzene, which is given in Figure 3c; the energy

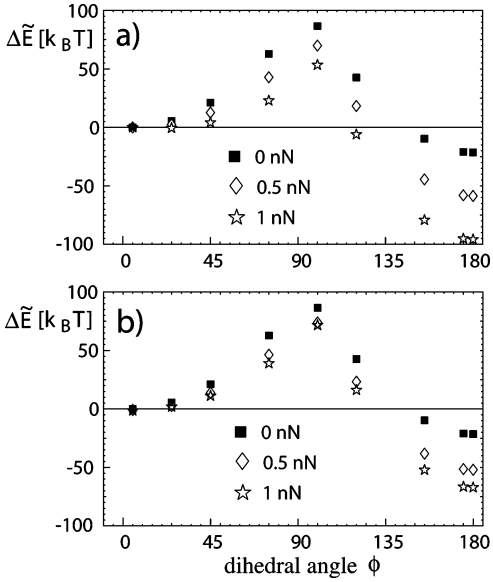

Figure 4. (a) The energy relative to the cis ground state as a function of the dihedral angle is plotted at forces corresponding to 0, 0.5, and 1 nN, according to eq 5. (b) Here, the elastic effects from Figure 3c are included via eq 6.

can then be written as

$$\Delta\tilde{E}(F) = \Delta E - (a[\phi] - a_{0,\mathrm{cis}})F - \frac{1}{2}a[\phi]F^2/\gamma_1[\phi] \tag{6}$$

Including elasticity effects changes the energy of the extended states considerably. In specific, the reduction of the barrier height under applied force is considerably reduced, which means that the conversion by rotation around the dihedral angle is not helped much by application of an external force.

Freely Rotating Chain Model. The molecules being studied are freely rotating molecules; therefore, we used the freely rotating chain (FRC) model to describe our polymers. The freely rotating chain (FRC) model consists of segments with fixed length b, called bond length, that are freely rotating at a fixed angle with respect to each other, as illustrated in the inset in Figure 5a.

The full force−distance relation is involved and has only recently been numerically determined. For high forces, the FRC model is asymptotically described by eq 7.[40]

$$\frac{R_z(F)}{L_0(N_\mathrm{p})} = 1 - \left(\frac{2Fb_\mathrm{p}}{k_\mathrm{B}T}\right)^{-1} \tag{7}$$

In this equation $R_z(F)$ is the chain length at given force F, $L_0(N_\mathrm{p}) = N_\mathrm{p}a_{\mathrm{p}0}/2$ is the contour length at zero force, k_B is the Boltzmann constant, T is the temperature, $a_{\mathrm{p}0}$ is the unit cell length that is used in the ab initio calculations at zero force, which comprises two peptide units, $a_{\mathrm{p}0}/2$ is the standard monomer length, and b_p is the bond length of a chemical bond. N_p refers to the number of monomers; since each monomer consists of a number of rotating bonds, N_p is not the number of rotating bonds in an equivalent FRC model.

In this study we fit the poly(azobenzene−peptide) by dividing it into three units: peptide, *trans*-azobenzene, and *cis*-azobenzene. Assuming that the behavior of the single units is additive, eq 7 was expanded as a sum over all units:

$$\frac{R_z(F,N_t,N_c)}{L_0(N_t,N_c)} = \sum_{i=1}^{3}\left(\frac{L_{i0}(N_t,N_c)}{L_0(N_t,N_c)}\left(1 - \left(\frac{2Fb_i}{k_\mathrm{B}T}\right)^{-1}\right)\right) \tag{8}$$

Here, $i = 1$ indicates peptide, $i = 2$ *trans*-azobenzene, and $i = 3$ *cis*-azobenzene. $L_0(N_t,N_c)$ is the contour lengths at zero force of the poly(azobenzene−peptide) (eq 9d). $L_{i0}(N_t,N_c)$ is the sum of all unit length at zero force from one species in the polymer (eqs 9a−9c).

The prefactor $L_{i0}(N_t,N_c)/L_0(N_t,N_c)$ is a weighting factor dependent on the amount of one species in the polymer.

Equation 8 includes now three different bond lengths b_i, namely the bond length for peptide $b_1 = b_p$, *trans*-azobenzene $b_2 = b_t$, and *cis*-azobenzene $b_3 = b_c$.

The contour length $L_0(N_t,N_c)$ of the poly(azobenzene−peptide) is separated into peptide $L_1 = L_{p0}(N_t,N_c)$, *trans*-azobenzene $L_2 = L_{t0}(N_t)$, and *cis*-azobenzene monomers $L_3 = L_{c0}(N_c)$:

$$L_1 = L_{p0}(N_p) = N_p a_{p0}/2 = (N_t + N_c)(5/3)a_{p0} \quad (9a)$$

$$L_2 = L_{t0}(N_t) = N_t a_{t0} \quad (9b)$$

$$L_3 = L_{c0}(N_c) = N_c a_{c0} \quad (9c)$$

$$L_0(N_t,N_c) = L_{p0}(N_t,N_c) + L_{t0}(N_t) + L_{c0}(N_c) \quad (9d)$$

Here a_{p0} is the peptide unit length at zero force (Figure 2a), a_{c0} is the *cis*-azobenzene unit length at zero force (Figure 2b), and a_{t0} is the *trans*-azobenzene unit length at zero force (Figure 2c). N_p, N_t, and N_c are the number of peptide, *trans*-azobenzene, and *cis*-azobenzene monomers, respectively. Note that by chemical synthesis, we have $N_p/2 = (N_t + N_c)(5/3)$. The unit lengths a_{c0}, a_{t0}, and a_{p0} are crystallographic values which have been verified with the ab initio calculations for *cis*-azobenzene, *trans*-azobenzene, and peptide[35] at zero force as illustrated in Figure 2 and described in eq 1.

Combined Freely Rotating Chain−Ab Initio Quantum Mechanical Model. In the combined FRC-ab initio QM (FRCQM) model, the unit length a_i is force dependent because $a_i(F)$ is the inverse function for the ab initio stretching force $F(a_i)$ as described in the ab initio section above (see eq 3).[35]

$$a_i(F) = F^{(-1)}(a_i) \quad (10)$$

Therefore, all the unit lengths become force dependent, and eqs 7−9 are rewritten as

$$\frac{R_z(F)}{L_0(N_p)} = \frac{L_0(F,N_p)}{L_0(N_p)}\left(1 - \left(\frac{2Fb_p}{k_BT}\right)^{-1}\right) \quad (11)$$

$$\frac{R_z(F,N_t,N_c)}{L_0(N_t,N_c)} = \sum_i \left(\frac{L_i(F,N_t,N_c)}{L_0(N_t,N_c)}\left(1 - \left(\frac{2Fb_i}{k_BT}\right)^{-1}\right)\right) \quad (12)$$

$$L_p(F,N_p) = N_p a_p(F)/2 = (N_t + N_c)(5/3)a_p(F) \quad (13a)$$

$$L_t(F,N_t) = N_t a_t(F) \quad (13b)$$

$$L_c(F,N_c) = N_c a_c(F) \quad (13c)$$

$$L_0(F,N_t,N_c) = L_p(F,N_t,N_c) + L_t(F,N_t) + L_c(F,N_c) \quad (13d)$$

For a standard freely rotating chain model where all bonds have the same lengths and the bond angles are identical, b is the length of one of those bonds. Since, however, the polymer backbone of peptide and also the azobenzene compounds is inhomogeneous, b has to be used as a fit parameter. The force-dependent unit lengths a_c, a_t, and a_p are determined by ab initio calculations, and therefore these are no fit parameters.

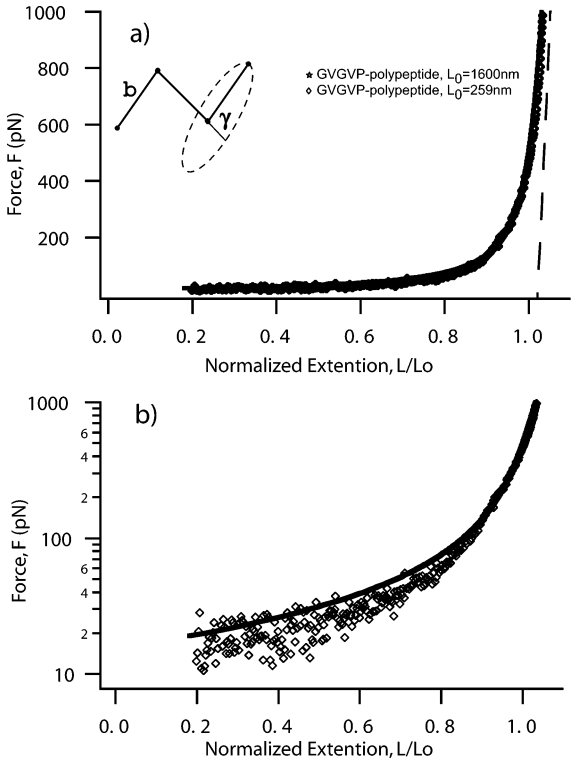

Figure 5. FRCQM fit (solid trace) and normalized force extension traces measured with two different chains (diamond and star) of the nonpolar poly-GVGVP. (a) The slope in the high force regime (>800 pN) of the two force vs extension curves were first fitted with the ab initio calculated elasticity for a dipeptide (long dash line). From this fit, the resulting contour length for the chains at zero force was determined to be $L_0 = 259$ nm (diamond) and $L_0 = 1600$ nm (star), respectively. These zero force contour lengths were used to normalize the measured curves. The ab initio elasticities combined with the FRC model (FRCQM) and a bond length of $b_p = 0.12$ nm were found to fit the low, medium, and high force range of the normalized experimental curves over the whole force range (solid line). Inset: geometric configuration of the FRC-model with segments of a fixed bond length, b, rotating freely around the bond axis at fixed angles γ.[40] (b) Semilogarithmic plot of the force as a function of the normalized extension L/L_0 for the experimental data (diamond) and the FRCQM fit (solid line).

With this combined FRCQM model the experimental force curves are fitted in the following way: The high force range of the nonpolar polypeptide chain was fitted first with the ab initio eq 13a. In this fit, only the number of monomers (peptides) was varied, and no bond length b_p was involved. From this fit the contour length at zero force and zero temperature was extracted ($L_0(F=0,N_p)$), and the force curves were normalized with this contour length.

Applying eq 11 to the normalized poly-GVGVP force curves results in the fitted bond length b_p, this length was later also used for the peptide bonds in the poly(azobenzene−peptide). At the same time the effects of fluctuations are taken into account (eq 11), which results in a length increase of the fitted contour length (Figure 5, solid line). Note: therefore, the dashed line in Figure 5 hits the x-axis at $L/L_0 > 1$.[35]

Following the procedure above, eq 13d was used to fit the high force range of the nonpolar poly(azobenzene−peptide) to extract the contour length at zero force and zero temperature. In this equation combinations of N_t and N_c were used to fit the high force range. The fit yields the number of *trans*-azobenzene and *cis*-azobenzene monomers.

To determine the difference between trans and cis due to optical switching, the number of azobenzene units was kept

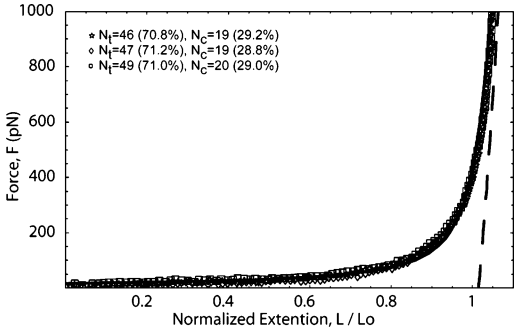

Figure 6. Poly(azobenzene−peptide) force curves compared with FRCQM prediction. Three force curves of nonpolar poly(azobenzene−peptide) containing about the same amount of *trans*- and *cis*-azobenzene are superimposed. Their good agreement shows that a change in curve shape does not result from uncertainties in the experiment (but reflects a switching of the polymers elasticity). The contour length L_0 for the polymer is extracted from the ab initio fit in the high force range (black dashed line). Now the number of azobenzene monomers in the trans and in the cis conformation can be calculated. The resulting FRCQM fit (solid line) uses the following bond lengths: *trans*-azobenzene (b_t = 0.11 nm), *cis*-azobenzene (b_c = 0.30 nm), and peptide (b_p = 0.12 nm).

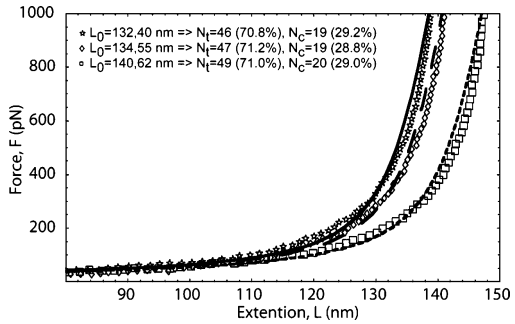

Figure 7. Nonnormalized force vs distance curves as used in Figure 6. The three curves from Figure 6 are fitted here with different contour length and the above calculated amount of azobenzene monomers in the trans and cis conformation. Short curve: data: star, fit: solid line; L_0 = 132.4 nm ⟨=⟩ N_t = 46 (70.8%), N_c = 19 (29.2%). Medium curve: data: diamond, fit: long dash line; L_0 = 134.55 nm ⟨=⟩ N_t = 47 (71.2%), N_c = 19 (28.8%) Long curve: data: square, fit: short dash line; L_0 = 140.62 nm ⟨=⟩ N_t = 49 (71.0%), N_c = 20 (29.0%).

constant ($N_t + N_c$ = costant), and only the ratio between trans and cis was varied (N_t/N_c = variable).

In the last step, the bond lengths for *trans*-azobenzene b_t and for *cis*-azobenzene b_c were ajusted to fit the whole force range for a wide range of conformational changes in the poly(azobenzene−peptide) (Figures 6−8).

Force curves shown in Figures 5−7 are selected on the basis of maximum force (to get a very precise L_0) and maximum polymer contour length (to have the elasticity of the polymer much smaller than the elasticity of the cantilever). The curves in Figure 8 were selected to demonstrate the FRCQM model over a large length change due to optical switching of the azobenzene monomers.

Results and Discussion

Since the poly(azobenzene−peptide) backbone predominantly consists of peptide bonds, the accuracy of the freely rotating chain−ab initio quantum mechanical (FRCQM) model was first demonstrated with a fit of the force−extension traces of two nonpolar polypeptide chains with different lengths (Figure 5). Following the procedure given above, the contour lengths were determined at zero force and zero temperature (see eq 13a, diamond, $L_0(F=0)$ = 259 nm, star, $L_0(F=0)$ = 1600 nm), and the experimental curves were normalized with these contour

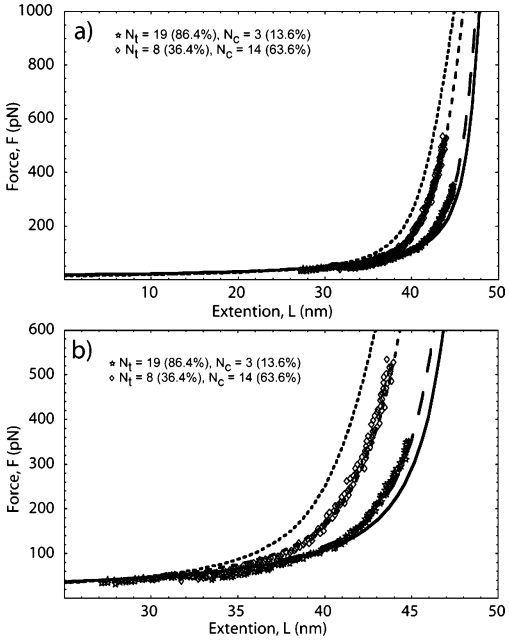

Figure 8. Light-induced switching of poly(azobenzene-peptide) compared to the theoretical prediction. (a) Experimentally observed optical switching of poly(azobenzene−peptide) from 86.4% trans (star) to 36.4% trans (diamond). The theoretical predicted FRCQM calculation is plotted for 86.4% trans (long dash line, N_t = 19, N_c = 3) and for 36.4% trans (short dash line, N_t = 8, N_c = 14). A theoretical all trans (solid line, N_t = 22, N_c = 0) and all cis (dotted line, N_t = 0, N_c = 22) conformation of the poly(azobenzene−peptide) is plotted to present the upper und lower limit for the length change. (b) Magnification of Figure 8a highlights the one-parameter fit and illustrates the excellent match between experiment and theory.

lengths and plotted on top of each other together with the theoretical curve based on the FRCQM model (eq 11, parameters from ref 35). The fit for the bond length b_p (Figure 5) gave a value of b_p = 0.12 nm, which is the unit-cell length divided by 6 and thus corresponds to the projected length per chemical bond. We fixed this value for all further fits of the poly(azobenzene−peptide). Note that there is no difference between the FJC and the FRC in the strong force regime if one treats b as a free fitting parameter.

Next, the ab initio quantum mechanical calculations at zero temperature for the azobenzene were performed as described above, resulting in free energies of the different azobenzene conformations as a function of their end-to-end distances (see Figure 1a). From these the molecular elasticities were derived and plotted in Figure 1b. This results in stretching moduli of γ_1 = 82.5 nN for the trans conformation and γ_1 = 2.02 nN for the cis conformation according to eq 4. The enormous difference in stretching modulus reflects the different architecture of the conformations: the trans conformation is straightened out, and any lengthening of the molecule either deforms the nitrogen bonds (which is costly), distorts the benzene rings, or changes the length of a bond. In the cis conformation, the total molecule is bent, and the force acting on the outer carbon atoms produces an enormous torque at the center. This means that not only the length per unit upon optical switching but also the elasticity of the polymer changes.

The transition between the cis and the trans state is visualized by the rotation around the dihedral angle ϕ at the nitrogen−nitrogen bond by 180°. As shown in Figure 3a, the cis-twisted geometry (denoted by squares) becomes instable at dihedral angles above roughly ϕ = 85°. Likewise, the trans conformation loses stability at angles below ϕ = 105°. In between, an intermediate structure appears. We have not been able to

determine the saddle point, which is probably caused by the near-degeneracy of many local minima close to the energy barrier.[67] Nevertheless, we estimate the barrier to be of the order of the energy of the cis and trans conformations where they almost cross.

In Figure 3b we plot the distance between the two outer carbon atoms as a function of the dihedral angle ϕ. At distances corresponding to the barrier state, the distance a is roughly intermediate between the unit cell size in the cis and trans conformations. This suggests that under an applied force the barrier height should be substantially decreased, and thus a mechanic pulling experiment should be able to induce the transition from the cis to the trans conformation at large enough forces. To test this, we plot in Figure 4a the force-dependent energy for forces corresponding to 0, 0.5, and 1 nN (cf. eq 5). It can be seen that the barrier height decreases from about 85 k_BT to about 55 k_BT. But if in addition, the angle dependence of the stretching modulus γ_1 (cf. Figure 3c) is included (according to eq 6), the barrier stays even above 70 k_BT (Figure 4b). This explains the, on first sight unexpected, high stability of the cis conformation against an external force, which was observed in the experiments.

This result can be generalized: pulling a soft molecule over a free energy barrier into a stiff state becomes increasingly difficult when the transition state is stiffer than the starting conformation. Conversely, it would be easy to push azobenzene from the trans conformation into the cis conformation.[60]

Comparing these calculated values for the barrier height with experimental results is not straightforward because the experimental analysis usually employs Kramer's theory, which strictly holds only in a one-dimensional configuration space for a reaction path; however, the actual path is in a multidimensional configuration space, and degrees of freedom that are orthogonal to the reaction path become important (e.g., translocational vibration which are characterized by the longitudinal stretching modulus γ_1; see Figure 3c). In addition, the ab initio calculation is performed with the very restrictive 6G basis set, and the saddle point of the transition is not determined. The values that can be extracted from the data in Figure 4 should therefore only be regarded as a rough estimate.

The main result of this project is highlighted in Figure 6. It shows three normalized force−extension traces measured on polymers of different lengths but equivalent cis-to-trans ratio of about 29:71 together with the predicted curve (solid line). These ratios and the total number of *cis*-azobenzene N_c and *trans*-azobenzene N_t are a result of the fit in the high force range (eq 13d); they result in the contour length at zero force.

As can be seen, the FRCQM model (eq 12) provides an excellent agreement between experiment and theory with a bond length $b_t = 0.11$ nm for *trans*-azobenzene and $b_c = 0.3$ nm for *cis*-azobenzene. Figure 7 shows the same curves but not normalized (star, solid fit: $L_0 = 132.40$ nm, $N_t = 46$, $N_c = 19$; diamond, long dash fit: $L_0 = 134.55$ nm, $N_t = 47$, $N_c = 19$; square, short dash fit: $L_0 = 140.62$ nm, $N_t = 49$, $N_c = 20$). In the Appendix we give some arguments why for polymers that consist of bonds with different lengths and different bond angles the effective bond length will tend to be smaller than the true bond length, in agreement with what we observed in our fits.

In Figure 8a this model was used to quantify the conversion ratio for a particular poly(azobenzene−peptide), which was switched back and forth optically. Two traces were picked and analyzed after the procedure given above. The best fit in the high force range was given for $N_t = 19$ and $N_c = 3$($N_t + N_c = 22$), resulting in a contour length of 45.9 nm (equation FRC 8d) and a trans-to-cis ratio of 86:14 (star, long dash line). After UV exposure it contracted into the state fitted best by the short dash line where the fraction of trans units was reduced to 36.4% ($N_t = 8$, $N_c = 14$, $N_t + N_c = 22$, $L_0 = 42.5$ nm, diamond, short dash line). The extremes of 0 and 100% conversion are shown as dotted ($N_t = 22$, $N_c = 0$, $L_0 = 46.8$ nm) and solid ($N_t = 0$, $N_c = 22$, $L_0 = 40.0$ nm) lines, respectively. Figure 8b is a magnification of Figure 8a and illustrates the large change from a most trans to the most cis conformation in the single molecule poly(azobenzene−peptide) experiment. This conversation rate is similar to the one observed in ensemble measurements.[68]

Conclusions

We have demonstrated that a new statistical model for the analysis of experimental force−extension data of poly(azobenzene−peptide)s can yield the precise number of units in the cis and trans conformation. The model is a combination of the freely rotating chain model and ab initio quantum mechanical calculations (FRCQM) for azobenzene and peptide units. The experimental data were analyzed in three steps. In the first step, force curves of nonpolar polypeptide chains were fitted with the FRCQM model and result in a bond length of $b_p = 0.12$ nm. In the second step, poly(azobenzene−peptide) force curves were fitted and resulted in bond lengths for *trans*-azobenzene of $b_t = 0.11$ nm and for *cis*-azobenzene of $b_c = 0.3$ nm. In the third step this parameter-free model was used to analyze the switching of the poly(azobenzene−peptide) from 86.4% trans to 36.4% trans.

As can be seen the model allows a one-parameter analysis of the degree of optical conversion and so for a determination of the quantum efficiency of the opto-mechanical transformation. Experiments of this kind in connection with these data analysis will be the basis of further development of the photonic muscle.

Beside the FRCQM model, the quantum mechanical calculations reveal that the forced conversion path is orthogonal or at least has no prominent collinear component to the thermal unfolding path. In other words, pulling at the ends of the azobenzene group does not help the rotation around the N−N double bond. As a result, the force acting along the polymer backbone does not reduce the remaining activation barrier for the thermal conformational transition, and as a consequence the force does not significantly reduce the lifetime of the cis conformation. This explains why the known thermal relaxation of the cis conformation within fractions of hours is not speeded to a time scale comparable to the force ramp in the experiment. This is why forces as high as 500 pN can be applied for many seconds to a mostly cis configuration without switching it to the trans conformation.

Acknowledgment. This work was supported by the Deutsche Forschungsgemeinschaft. Helpful discussions with Markus Seitz and Dan Urry are gratefully acknowledged. The azo-polymers were kindly provided by Louis Moroder.

Appendix. High-Force Limit of Freely Rotating Chain Model

We present here a generalization of the scaling arguments already displayed in a previous publication.[69] Consider a freely rotating chain model under large extensional forces. In this high force limit, the chain will adopt an extended conformation, and we only consider small librational fluctuations around this ground state. In the previous publication, all bonds had the same lengths and bond angles. Now, we show a slightly more general model where the chain consists of two bonds of different lengths

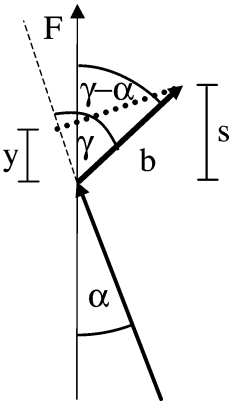

Figure 9. High-force limit of freely rotating chain model. Shown is a general model where the chain consists of two bonds of different length and in principle also of different bond angle. The upper bond makes an angle γ with the lower bond and an angle $\gamma-\alpha$ with the vertical axis. The torsional angle ϕ determines angular fluctuations away from the ground state, where $y = b \cos\gamma \cos\alpha$ and $s = b \cos(\gamma-\alpha)$ and b is the bond length.

and in principle also of different bond angle. Figure 9 depicts two bonds that might make up the chain and all the relevant variables.

The vertical axis denotes the direction along which the external force acts. The upper bond (the vertical orientation of which we want to calculate) makes an angle γ with the lower bond and an angle $\gamma-\alpha$ with the vertical axis. The torsional angle ϕ determines angular fluctuations away from the ground state. The projected length along the force direction is given by

$$z = y + (s - y)\cos\phi$$

where $y = b\cos\gamma\cos\alpha$ and $s = b\cos(\gamma - \alpha)$ and b is the bond length. The fluctuation of the upper bond is determined by the partition function

$$Z = \int_0^{2\pi} \mathrm{d}\phi \exp\{zF/k_BT\} \approx \sqrt{2\pi k_BT/(F(s-y))}\exp(Fs/k_BT)$$

from which the vertical extension follows by a partial derivative as $\langle z\rangle = \partial \ln Z/\partial(F/k_BT)$. Dividing the vertical extension $\langle z\rangle$ by the projected bond length s, we obtain finally

$$\frac{\langle z\rangle}{s} = 1 - \frac{k_BT}{2Fb\cos(\gamma-\alpha)}$$

The new result is the factor $\cos(\gamma-\alpha)$, which amounts to a reduction of the effective bond length by a geometric factor. A bond that is oriented closely to the force axis will only be subject to a small correction, but for bonds that are oriented at a large angle $\gamma-\alpha$ away from the force axis the correction term will be important. The main result is that the effective bond length will be reduced, and this effect might be especially important for polymers, which consist of bonds of different lengths and different bond angles. This observation is in accord with the results obtained in this paper based on the fits of experimental data, where the effective bond lengths were found to be substantially smaller than the geometric bond lengths obtained within the ab initio calculation. An explanation could be that some of the bonds make large angles with the force axis.

Note Added after ASAP Publication. This article was published ASAP on December 15, 2005. For the sake of consistency, the character *f* has been changed to *F* from eq 7 to the end of the paper. The correct version was posted on December 28, 2005.

References and Notes

(1) Rief, M.; Gautel, M.; Oesterhelt, F.; Fernandez, J. M.; Gaub, H. E. *Science* **1997**, *276*, 1109−1112.
(2) Rief, M.; Fernandez, J. M.; Gaub, H. E. *Phys. Rev. Lett.* **1998**, *81*, 4764−4767.
(3) Oesterhelt, F.; Oesterhelt, D.; Pfeiffer, M.; Engel, A.; Gaub, H. E.; Muller, D. J. *Science* **2000**, *288*, 143−146.
(4) Kessler, M.; Gaub, H. E. *Nat. Struct. Mol. Biol.*, submitted.
(5) Kellermayer, M. S. Z.; Smith, S. B.; Granzier, H. L.; Bustamante, C. *Science* **1997**, *276*, 1112−1116.
(6) Rief, M.; Clausen-Schaumann, H.; Gaub, H. E. *Nat. Struct. Biol.* **1999**, *6*, 346−349.
(7) Smith, S. B.; Finzi, L.; Bustamante, C. *Science* **1992**, *258*, 1122.
(8) Bustamante, C.; Smith, S. B.; Liphardt, J.; Smith, D. *Curr. Opin. Struct. Biol.* **2000**, *10*, 279−285.
(9) Clausen-Schaumann, H.; Rief, M.; Gaub, H. E. *Biophys. J.* **1999**, *76*, A151−A151.
(10) Albrecht, C.; Blank, K.; Lalic-Multhaler, M.; Hirler, S.; Mai, T.; Gilbert, I.; Schiffmann, S.; Bayer, T.; Clausen-Schaumann, H.; Gaub, H. E. *Science* **2003**, *301*, 367−370.
(11) Bockelmann, U. *Curr. Opin. Struct. Biol.* **2004**, *14*, 368−373.
(12) Allemand, J. F.; Bensimon, D.; Croquette, V. *Curr. Opin. Struct. Biol.* **2003**, *13*, 266−274.
(13) Bouchiat, C.; Wang, M. D.; Allemand, J.-F.; Strick, T.; Block, S. M.; Croquette, V. *Biophys. J.* **1999**, *76*, 409−413.
(14) Hugel, T.; Seitz, M. *Macromol. Rapid Commun.* **2001**, *22*, 989−1016.
(15) Hugel, T.; Holland, N. B.; Cattani, A.; Moroder, L.; Seitz, M.; Gaub, H. E. *Science* **2002**, *296*, 1103−1106.
(16) Holland, N. B.; Hugel, T.; Neuert, G.; Cattani-Scholz, A.; Renner, C.; Oesterhelt, D.; Moroder, L.; Seitz, M.; Gaub, H. E. *Macromolecules* **2003**, *36*, 2015−2023.
(17) Urry, D. W.; Hugel, T.; Seitz, M.; Gaub, H. E.; Sheiba, L.; Dea, J.; Xu, J.; Parker, T. *Philos. Trans. R. Soc. London, Ser. B: Biol. Sci.* **2002**, *357*, 169−184.
(18) Rief, M.; Oesterhelt, F.; Heymann, B.; Gaub, H. E. *Science* **1997**, *275*, 1295−1297.
(19) Friedsam, C.; Becares, A. D.; Jonas, U.; Seitz, M.; Gaub, H. E. *New J. Phys.* **2004**, *6*.
(20) Friedsam, C.; Seitz, M.; Gaub, H. E. *J. Phys.: Condens. Matter* **2004**, *16*, S2369−S2382.
(21) Seitz, M.; Friedsam, C.; Jostl, W.; Hugel, T.; Gaub, H. E. *ChemPhysChem* **2003**, *4*, 986−990.
(22) Ashkin, A.; Schütze, K.; Dziedzic, J. M.; Euteneuer, U.; Schliwa, M. *Nature (London)* **1990**, *348*, 346.
(23) Bustamante, C.; Bryant, Z.; Smith, S. B. *Nature (London)* **2003**, *421*, 423−427.
(24) Neuman, K. C.; Block, S. M. *Rev. Sci. Instrum.* **2004**, *75*, 2787−2809.
(25) Lang, M. J.; Fordyce, P. M.; Engh, A. M.; Neuman, K. C.; Block, S. M. *Nat. Methods* **2004**, *1*, 133−139.
(26) Sheetz, M. P., Ed.; *Laser Tweezers in Cell Biology*; Academic Press: New York, 1997.
(27) Merkel, R.; Nassoy, P.; Leung, A.; Ritchie, K.; Evans, E. *Nature (London)* **1999**, *397*, 50−53.
(28) Evans, E. *Annu. Rev. Biophys. Biomol. Struct.* **2001**, *30*, 105−128.
(29) Evans, E.; Ritchie, K. *Biophys. J.* **1997**, *72*, 1541−1555.
(30) Clausen-Schaumann, H.; Seitz, M.; Krautbauer, R.; Gaub, H. E. *Curr. Opin. Chem. Biol.* **2000**, *4*, 524−530.
(31) Gaub, H. E. *Abstr. Pap. Am. Chem. Soc.* **2000**, *220*, U260−U260.
(32) Grandbois, M.; Beyer, M.; Rief, M.; Clausen-Schaumann, H.; Gaub, H. E. *Science* **1999**, *283*, 1727−1730.
(33) Rief, M.; Grubmuller, H. *ChemPhysChem* **2002**, *3*, 255−261.
(34) Oesterhelt, F.; Rief, M.; Gaub, H. E. *New J. Phys.* **1999**, *1*, 6.1.
(35) Hugel, T.; Rief, M.; Seitz, M.; Gaub, H. E.; Netz, R. R. *Phys. Rev. Lett.* **2005**, *94*.
(36) Krautbauer, R.; Pope, L. H.; Schrader, T. E.; Allen, S.; Gaub, H. E. *FEBS Lett.* **2002**, *510*, 154−158.
(37) Krautbauer, R.; Rief, M.; Gaub, H. E. *Nano Lett.* **2003**, *3*, 493−496.
(38) Hugel, T.; Grosholz, M.; Clausen-Schaumann, H.; Pfau, A.; Gaub, H.; Seitz, M. *Macromolecules* **2001**, *34*, 1039−1047.
(39) Odijk, T. *Macromolecules* **1995**, *28*, 7016−7018.
(40) Livadaru, L.; Netz, R. R.; Kreuzer, H. J. *Macromolecules* **2003**, *36*, 3732−3744.
(41) Friedsam, C.; Wehle, A. K.; Kühner, F.; Gaub, H. E. *J. Phys.: Condens. Matter* **2003**, *15*, S1709−S1723.
(42) Kreuzer, H. J.; Wang, R. L. C.; Grunze, M. *New J. Phys.* **1999**, *21*, 1367−2630.
(43) Livadaru, L.; Netz, R. R.; Kreuzer, H. J. *J. Chem. Phys.* **2003**, *118*, 1404−1416.

(44) Netz, R. R. *Macromolecules* **2001**, *34*, 7522−7529.
(45) Rohrig, U. F.; Troppmann, U.; Frank, I. *Chem. Phys.* **2003**, *289*, 381−388.
(46) Rohrig, U. F.; Frank, I. *J. Chem. Phys.* **2001**, *115*, 8670−8674.
(47) Finkelmann, H.; Nishikawa, E.; Pereira, G. G.; Warner, M. *Phys. Rev. Lett.* **2001**, *87*, 015501.
(48) Brown, C. H., Ed. *Photochromism*; Wiley-Interscience: New York, 1971.
(49) Tamai, N.; Miyasaka, H. *Chem. Rev.* **2000**, *100*, 1875.
(50) Irie, M. In *Photoreactive Materials for Ultrahigh-Density Optical Memory*; Irie, M., Ed.; Elsevier: Amsterdam, 1994; p 1.
(51) Rau, H. In *Photochromism: Molecules and Systems*; Dürr, H., Bouas-Laurent, H., Eds.; Elsevier: Amsterdam, 1990; Chapter 4.
(52) Rau, H. *J. Photochem.* **1984**, *26*, 221.
(53) Shinkai, S.; Manabe, O. *Top. Curr. Chem.* **1984**, *121*, 67−104.
(54) Willner, I. *Acc. Chem. Res.* **1997**, *30*, 347−356.
(55) Archut, A.; Vögtle, F.; De Cola, L.; Azzellini, G. C.; Balzani, V.; Ramanujam, P. S.; Berg, R. H. *Chem.—Eur. J.* **1998**, *4*, 699−706.
(56) Strzegowski, L. A.; Martinez, M. B.; Gowda, D. C.; Urry, D. W.; Tirrell, D. A. *J. Am. Chem. Soc.* **1994**, *116*, 813−814.
(57) Lagungé Labarthet, F.; Bruneel, J. L.; Buffeteau, T.; Sourisseau, C.; Huber, M. R.; Zilker, S. J.; Bieringer, T. *Phys. Chem. Chem. Phys.* **2000**, *2*, 5154−5167.
(58) Feringa, B. L.; Jager, W. F.; de Lange, B.; Meijer, E. W. *J. Am. Chem. Soc.* **1991**, *113*, 5468−5470.
(59) Feringa, B. L.; van Delden, R. A.; Koumura, N.; Geertsema, E. M. *Chem. Rev.* **2000**, *100*, 1789−1816.
(60) Monti, S.; Orlandi, G.; Palmieri, P. *Chem. Phys.* **1982**, *71*, 87.
(61) Behrendt, R.; Renner, C.; Schenk, M.; Wang, F.; Wachtveitl, J.; Oesterhelt, D.; Moroder, L. *Angew. Chem., Int. Ed.* **1999**, *38*, 2771−2773.
(62) Binnig, G.; Quate, C. F.; Gerber, C. *Phys. Rev. Lett.* **1986**, *56*, 930.
(63) Butt, H. J.; Jaschke, M. *Nanotechnology* **1995**, *6*, 1−7.
(64) Kreuzer, H. J.; Grunze, M. *Europhys. Lett.* **2001**, *55*, 640−646.
(65) Adamson, A. W.; Vogler, A.; Kunkely, H.; Wachter, R. *J. Am. Chem. Soc.* **1978**, *100*, 1298.
(66) Nerbonne, J. M.; Weiss, R. J. *J. Am. Chem. Soc.* **1978**, *100*, 5953.
(67) Frank, I., to be published.
(68) Renner, C.; Cramer, J.; Behrendt, R.; Moroder, L. *Biopolymers* **2000**, *54*, 501−514.
(69) Aktah, D.; Frank, I. *J. Am. Chem. Soc.* **2002**, *124*, 3402−3406.

MA051622D